Constructing Synergistic Triazine and Acetylene Cores in Fully Conjugated Covalent Organic Frameworks for Cascade Photocatalytic H_2O_2 Production

Lipeng Zhai,[†ǂ] Zhipeng Xie,[‡ǂ] Cheng-Xing Cui,[//ǂ] Xiubei Yang,[†] Qing Xu,[§*] Xiating Ke,[‡] Minghao Liu,[§] Ling-Bo Qu,[I] Xiong Chen,[‡*] Liwei Mi*

†: Henan Key Laboratory of Functional Salt Materials, Center for Advanced Materials Research, Zhongyuan University of Technology, Zhengzhou 450007, P. R. China
‡: State Key Laboratory of Photocatalysis on Energy and Environment, and Key Laboratory of Molecular Synthesis and Function Discovery, College of Chemistry, Fuzhou University, Fuzhou 350116 P. R. China
§: CAS Key Laboratory of Low-Carbon Conversion Science and Engineering, Shanghai Advanced Research Institute (SARI), Chinese Academy of Sciences (CAS), Shanghai 201210, P. R. China
ǁ: School of Chemistry and Chemical Engineering, Henan Institute of Science and Technology, Xinxiang 453003 P. R. China
I: College of Chemistry, and Institute of Green Catalysis, Zhengzhou University, Zhengzhou 450001 P. R. China
ǂ: L. Zhai, Z. Xie, and C.-X. Cui contributed equally to this work.

Corresponding Author

*xuqing@sari.ac.cn, *chenxiong987@fzu.edu.cn, *mlwzzu@163.com

Contents

Section A. Materials and Methods

Section B. Experimental Procedures

Section C. Results and Discussion

Section D. References

Section A. Materials and Methods

Characterization. ^{1}H NMR spectra were measured on a Bruker 400 MHz spectrometer, while chemical shifts (δ in ppm) were determined using a standard of the solvent residual proton. Fourier transform infrared (FT-IR) spectra were recorded on a JASCO model FT IR-6100 infrared spectrometer. Powder X-ray diffraction (XRD) data were recorded on a Bruker D8 Focus Powder X-ray Diffractometer by using powder on glass substrate, from $2\theta = 1.5°$ up to 30° with 0.01° increment. Elemental analysis was performed on an Elementar vario MICRO cube elemental analyzer. TGA measurements were performed on a Discovery TGA under N_2, by heating from 30 to 800 °C at a rate of 10 °C min^{-1}. Nitrogen sorption isotherms were measured at 77 K with a TriStar II instrument (Micromeritics). The Brunauer-Emmett-Teller (BET) method was utilized to calculate the specific surface areas. By using the non-local density functional theory (NLDFT) model, the pore volume was derived from the sorption curve. Morphology images were characterized with a Zeiss Merlin Compact filed emission scanning electron microscope (FE-SEM) equipped with an energy-dispersive X-ray spectroscopy (EDS) system at an electric voltage of 5 KV.

Photocatalytic H_2O_2 production experiments. Typically, 10 mg of as-synthesized COF powder was dispersed in 2.5 mL EtOH/H_2O (EtOH 0.25 mL and H_2O 2.25 mL) solution in a Schlenk flask (10 mL). The suspension solutions were stirred for 10 min in the dark with continuous O_2 bubbling after ultrasound treatment for a few mins to reach the absorption-desorption equilibrium. The reaction temperature was kept at 25 °C with a circulating water bath. A 50 W LED lamp (~ 420 nm) was used as the light source. The concentration of H_2O_2 was determined by a UV spectrophotometer after removal of the photocatalyst with centrifuging at 10000 rpm followed by filtration with a 0.1 μm filter in the dark.

Computational calculations. Saturated cluster model of EBA-COF and BTEA-COF were used as the model system during the whole calculations. The functional of cam-B3-LYP were adopted along with 6-31G(d) basis set. Semiclassical dispersion corrections were with GD3BJ in all calculations.[S1] The geometrical structures were full optimized without any restrictions and frequency calculations were further performed to confirmed that located intermediates are real local minimums. All calculations were performed with Gaussian 16. The DOS and partial DOS (PDOS) were obtained with Multiwfn.[S2]

Materials. 2,4,6-trimethyl-1,3,5-triazine (TM), 4,4'-(ethyne-1,2-diyl) dibenzaldehyde (EBA) and 4,4',4''-(benzene-1,3,5-triyltris(ethyne-2,1-diyl)) tribenzaldehyde (BTEA) were prepared using reported methods.[S3-S5] Trifluoroacetic acid (TFA), 1,3,5-trimethylbenzene, 1,4-dioxene, acetonitrile, methanol, ammonia solution, dichloromethane, and tetrahydrofuran (THF) were purchased from Aladdin Chemicals. All the other solvents were purchased from Aladdin Chemicals and used as received without further purification.

Section B. Experimental Procedures

Synthesis of EBA-COF: A Pyrex tube (10 mL) was charged with 2,4,6- trimethyl-1,3,5-triazine (TM, 12.32 mg, 0.1 mmol), 4,4'-(ethyne-1,2-diyl) dibenzaldehyde (EBA, 35.14 mg, 0.15 mmol), 0.9 mL mesitylene, 0.9 mL 1,4-dioxane, 0.40 mL trifluoroacetic acid, and 50 μL acetonitrile. The tube was then flash frozen at 77 K and degassed by three freeze-pump-thaw cycles. The tube was sealed and heated at 150 °C for 3 days. The collected powder was neutralized by 0.1 mol L^{-1} NH_4OH solution in aqueous methanol (50 wt%) and washed with THF and methanol. The solid was then washed with methanol in a Soxhlet extractor for another 12 h. Subsequently, the product was dried at 120 °C under vacuum for 12 h to obtain the corresponding yellow powder in ~85% isolated yield.

Synthesis of BTEA-COF: A Pyrex tube (10 mL) was charged with 2,4,6- trimethyl-1,3,5-triazine (TM, 12.3 mg, 0.1 mmol), 4,4',4''-(benzene-1,3,5-triyltris(ethyne-2,1-diyl)) tribenzaldehyde ((BTEA, 46.25 mg, 0.1 mmol), 0.9 mL mesitylene, 0.9 mL 1,4-dioxane, 0.40 mL trifluoroacetic acid, and 50 μL acetonitrile. The tube was then flash frozen at 77 K and degassed by three freeze-pump-thaw cycles. The tube was sealed and heated at 150 °C for 3 days. The collected powder was neutralized with 0.1 mol L^{-1} NH_4OH solution in aqueous methanol (50 wt%) and washed with THF and methanol. The solid was then washed with methanol in a Soxhlet extractor for another 12 h. The product was then dried at 120 °C under vacuum for 12 h to obtain the corresponding yellow powder in ~87% isolated yield.

Section C. Results and Discussion

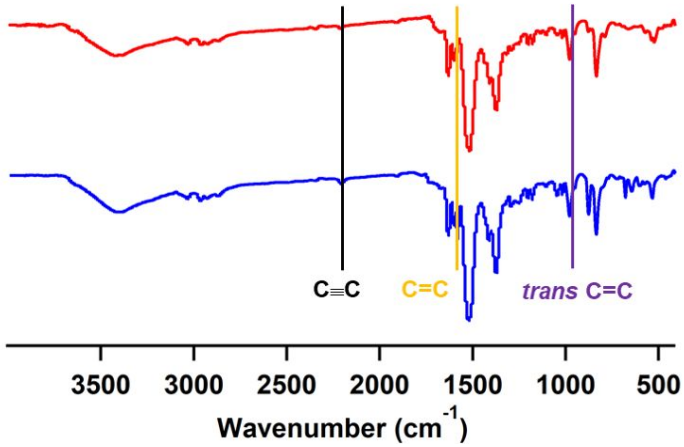

Figure S1. FT-IR spectra of EBA-COF (red) and BTEA-COF (blue).

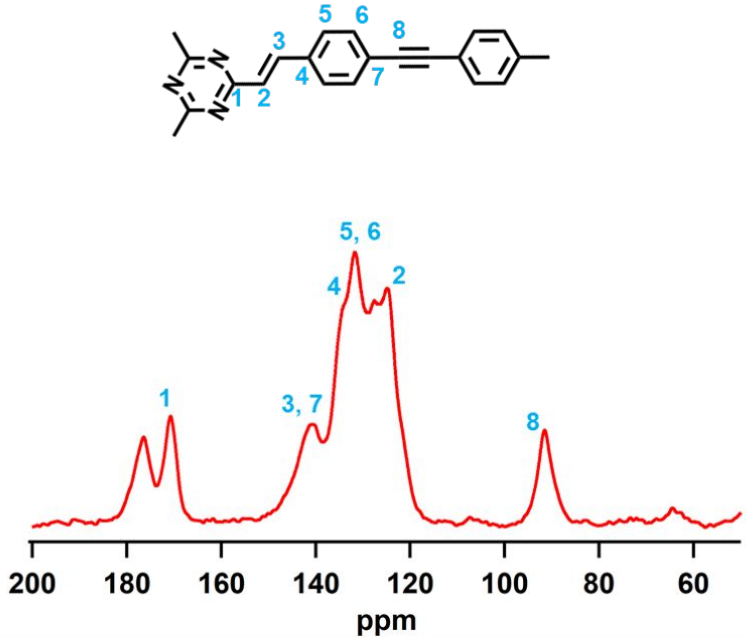

Figure S2. Solid State ^{13}C CP-MAS NMR spectrum of EBA-COF.

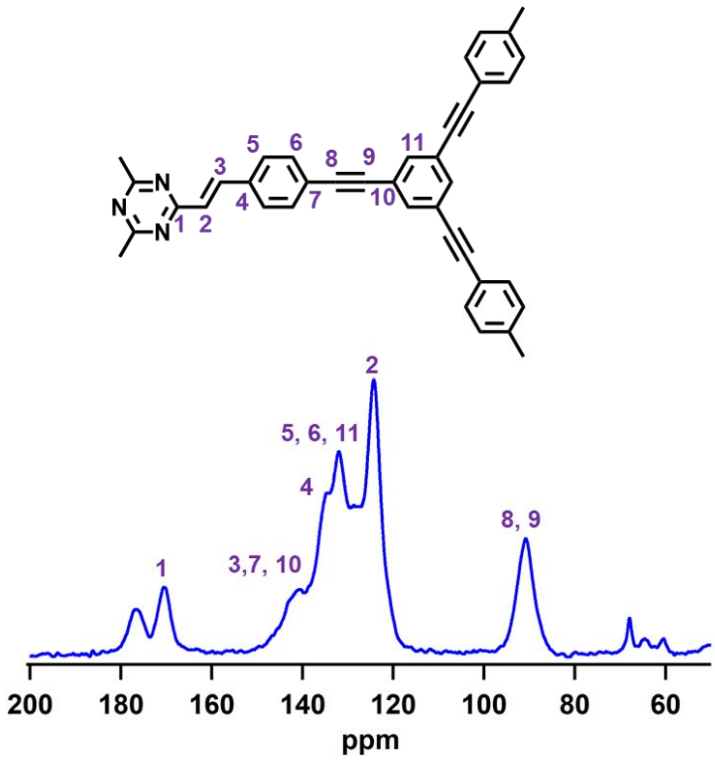

Figure S3. Solid State ^{13}C CP-MAS NMR spectrum of BTEA-COF.

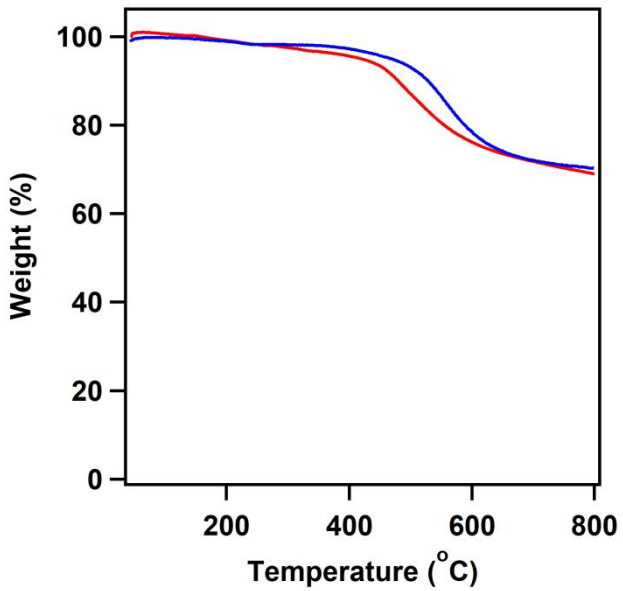

Figure S4. Thermogravimetric curves of EBA-COF (red) and BTEA-COF (blue) in N_2.

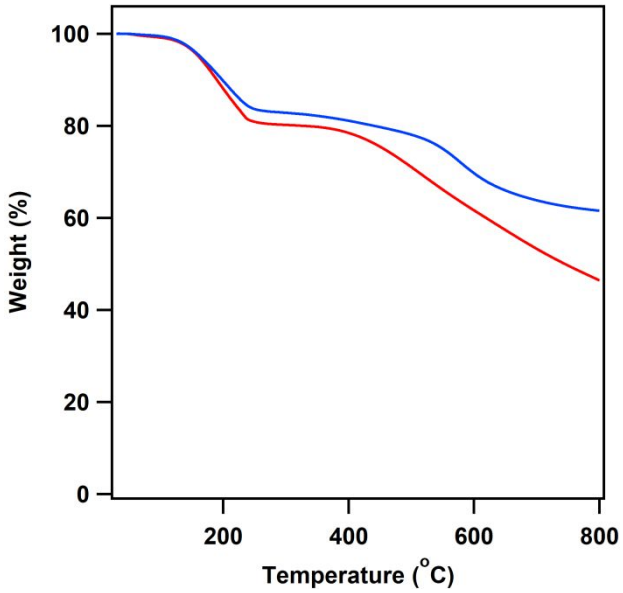

Figure S5. Thermogravimetric curves of EBA-COF (red) and BTEA-COF (blue) in air.

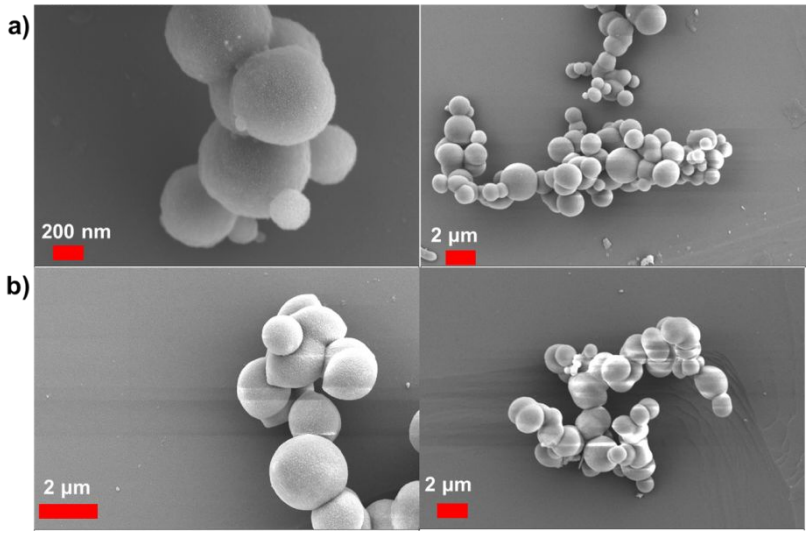

Figure S6. SEM images of (a) EBA-COF and (b) BTEA-COF.

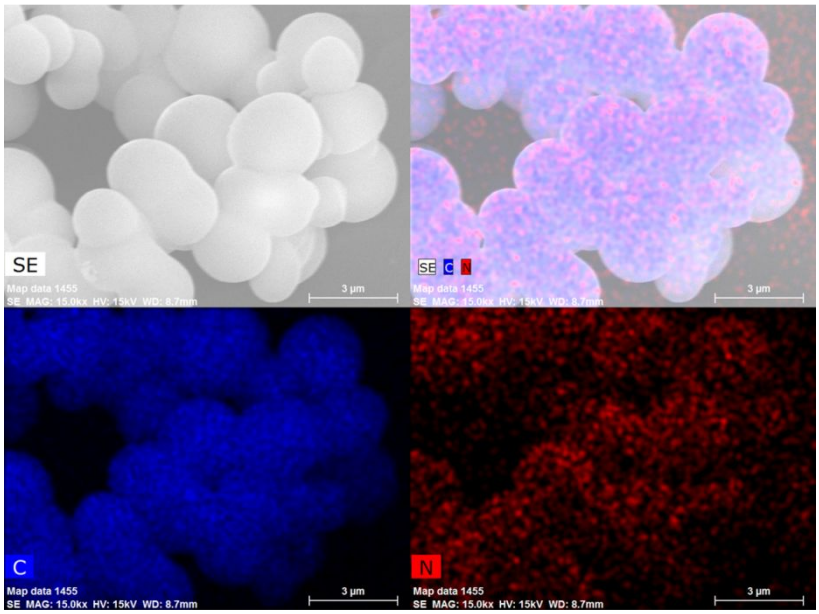

Figure S7. Elemental mapping images of EBA-COF using silicon as substrate.

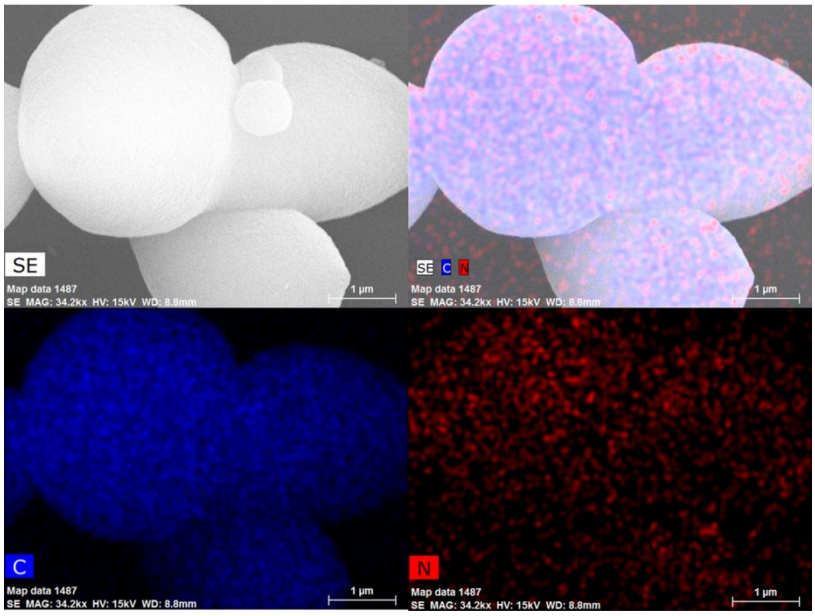

Figure S8. Elemental mapping images of BTEA-COF using silicon as substrate.

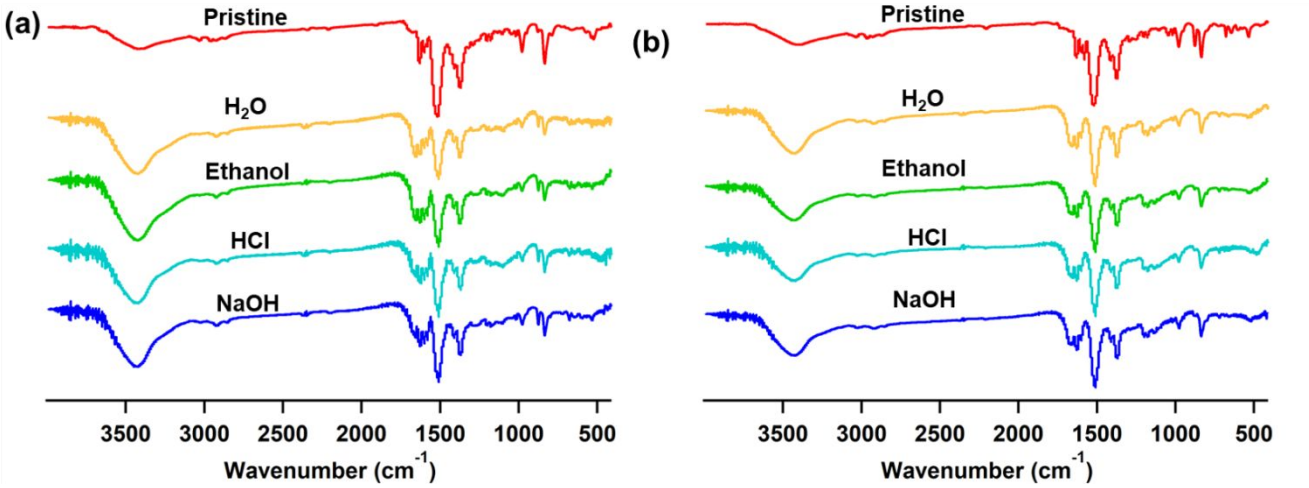

Figure S9. FT-IR spectra of BTEA-COF (a) and EBA-COF (b) after treatment with different solvents including H_2O, ethanol, HCl (1M), and NaOH (1M) at room temperature after 3 days.

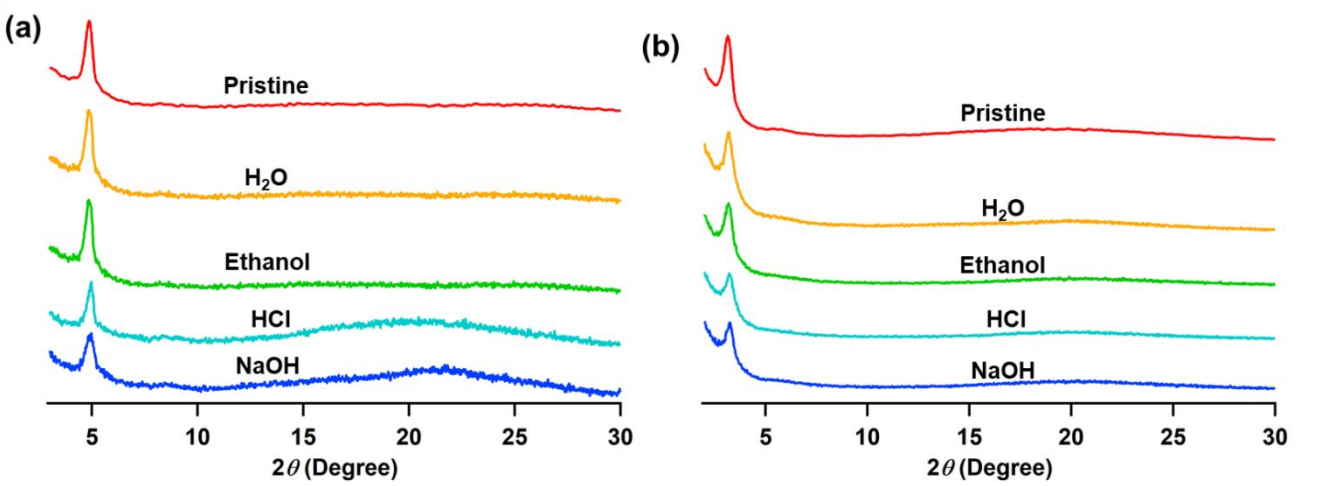

Figure S10. PXRD curves of BTEA-COF (a) and EBA-COF (b) after treatment with different solvents including H_2O, ethanol, HCl (1M), and NaOH (1M) at room temperature after 3 days.

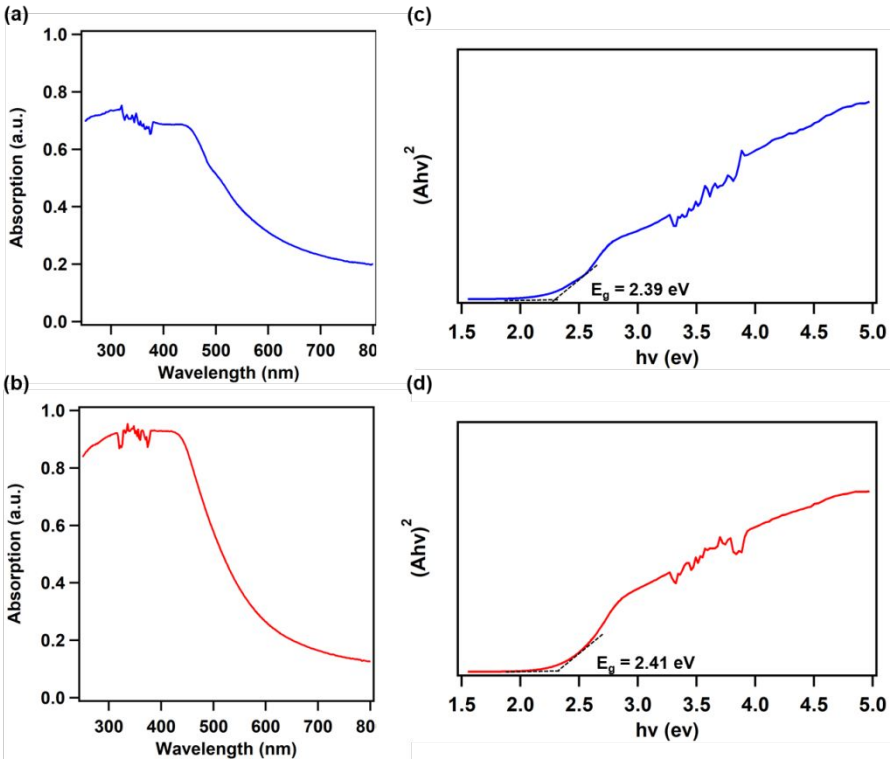

Figure S11. UV−vis diffuse reflectance spectra of (a) EBA-COF and (b) BTEA-COF. Tauc plots and optical images of (c) EBA-COF and (d) BTEA-COF.

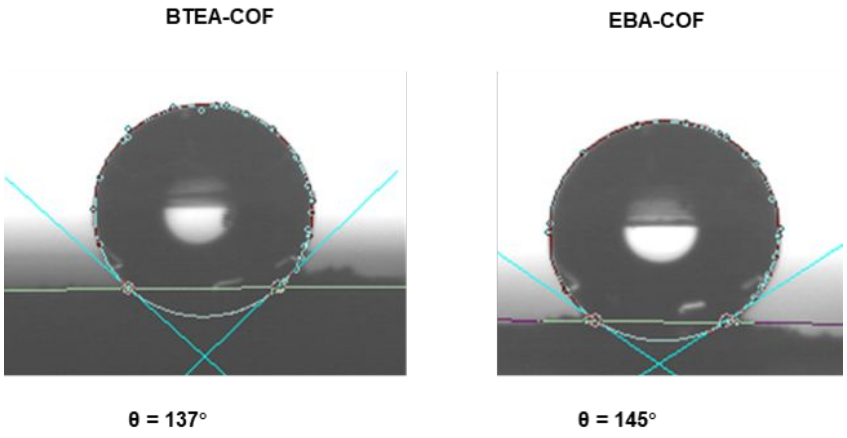

Figure S12. The contact angle of water on BTEA-COF and EBA-COF.

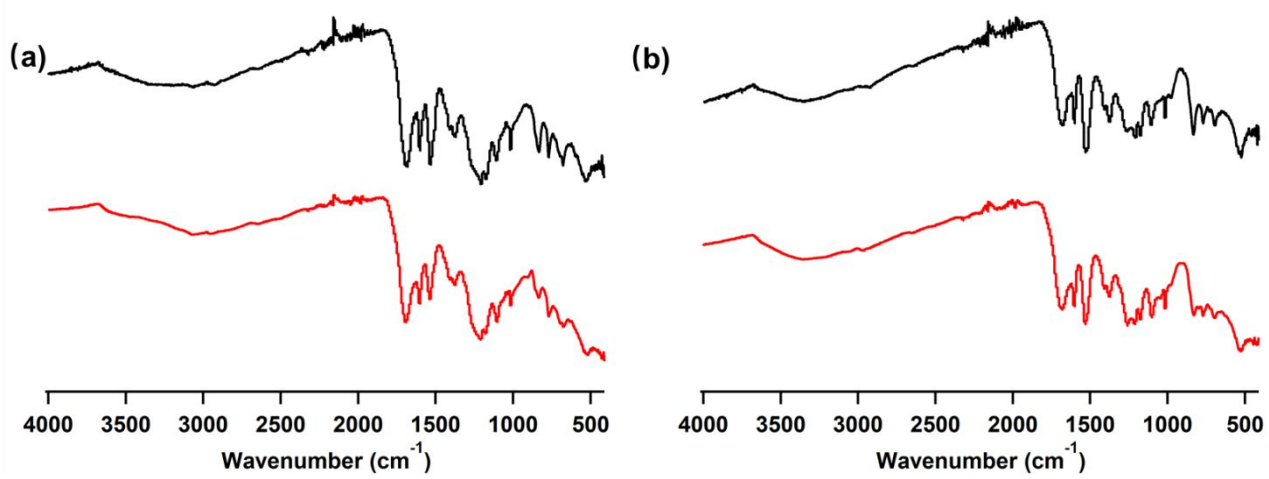

Figure S13. FT-IR spectra of BTEA-COF (a) and EBA-COF (b) before (red) and after the photocatalytic experiment (black).

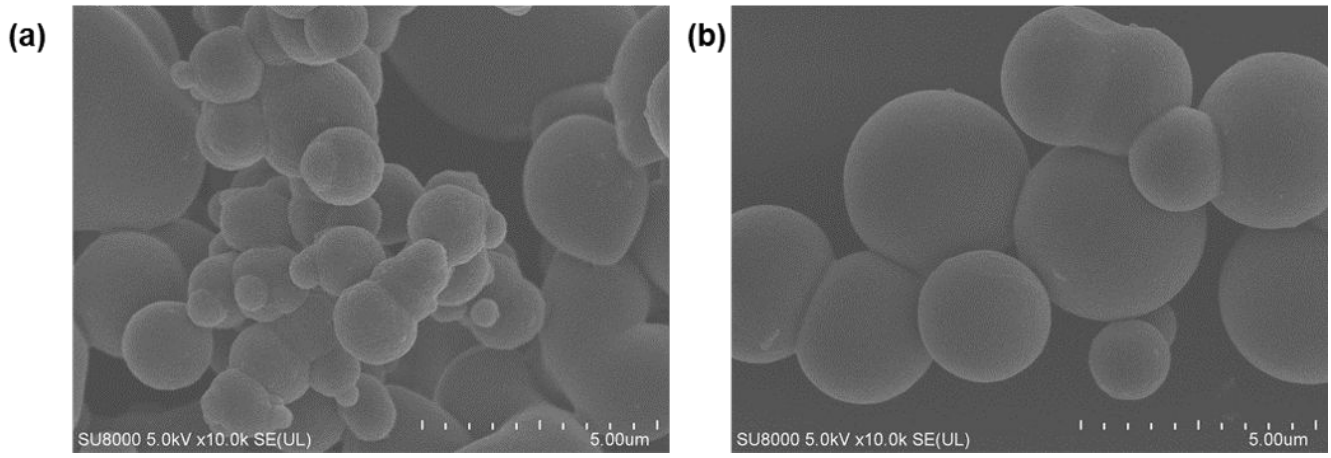

Figure S14. SEM images of BTEA-COF (a) and EBA-COF (b) after the photocatalytic experiment.

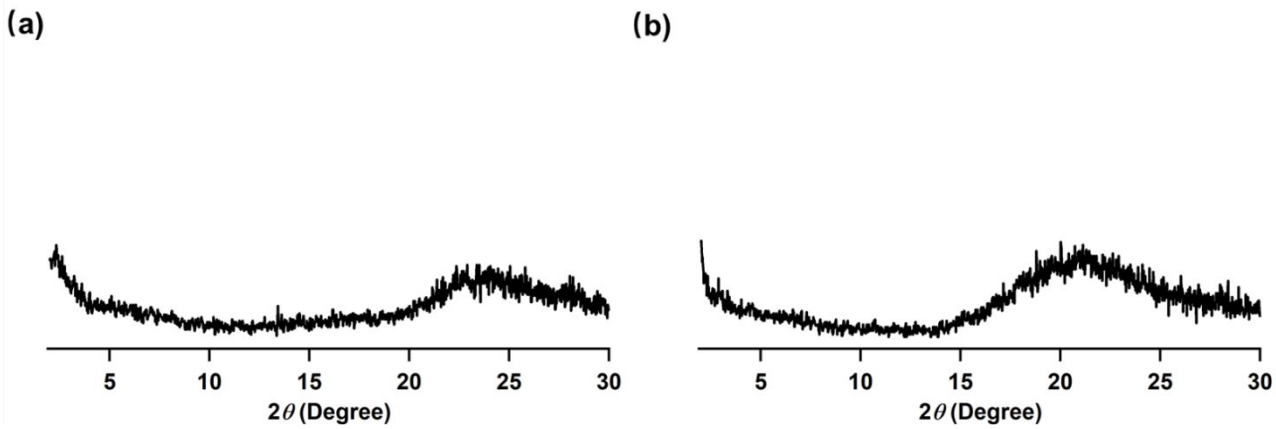

Figure S15. PXRD curves of BTEA-COF (a) and EBA-COF (b) after the photocatalytic experiment.

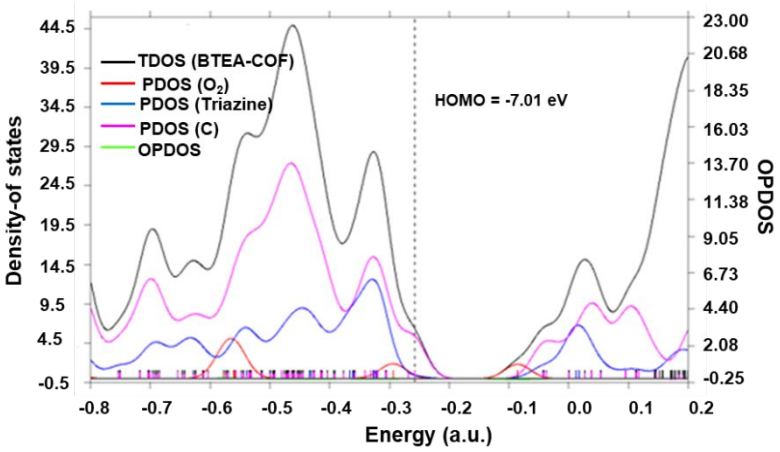

Figure S16. The total density of state (TDOS) of the model system of BTEA-COF and the partial DOS of O_2, triazine, and carbon atoms.

Table S1. Elemental analysis of DCTMP-DMTP-COF.

		C (%)	H (%)	N (%)
EBA-COF	Calcd.	85.71	4.29	10.00
	Found	84.23	4.61	10.14
BTEA-COF	Calcd.	88.14	3.95	7.91
	Found	87.86	4.02	8.05

Table S2. Atomistic coordinates for the AA-stacking mode of EBA-COF optimized using DFTB$^+$ method. Lattice type: Hexagonal, Space group: P6/M; $\alpha = \beta = 90°$, $\gamma = 120°$, a = 34.3767 Å, b = 34.3767 Å, c = 3.5355 Å.

N1	N	0.68447	0.30593	0.5	Uiso	1
C2	C	0.71198	0.35113	0.5	Uiso	1
C3	C	0.60897	0.23926	0.5	Uiso	1
C4	C	0.62443	0.21068	0.5	Uiso	1
C5	C	0.56707	0.40532	0.5	Uiso	1
C6	C	0.59438	0.45227	0.5	Uiso	1
C7	C	0.57499	0.4796	0.5	Uiso	1
C8	C	0.52827	0.46018	0.5	Uiso	1
C9	C	0.50095	0.41346	0.5	Uiso	1
C10	C	0.52034	0.38613	0.5	Uiso	1
C11	C	0.50836	0.48821	0.5	Uiso	1
H12	H	0.57104	0.22481	0.5	Uiso	1
H13	H	0.66217	0.22393	0.5	Uiso	1
H14	H	0.63249	0.46809	0.5	Uiso	1
H15	H	0.59728	0.51771	0.5	Uiso	1
H16	H	0.46284	0.39764	0.5	Uiso	1
H17	H	0.49804	0.34802	0.5	Uiso	1

Table S3. Atomistic coordinates for the AA-stacking mode of BTEA-COF optimized using DFTB$^+$ method. Lattice type: Hexagonal, Space group: P/6; $\alpha = \beta = 90°$, $\gamma = 120°$, $a = 23.1146$ Å, $b = 23.1146$ Å, $c = 3.5350$ Å.

N1	N	0.30528	0.70604	0.5	Uiso	1
C2	C	0.26575	0.63862	0.5	Uiso	1
C3	C	0.39072	0.58373	0.5	Uiso	1
C4	C	0.45649	0.6083	0.5	Uiso	1
C5	C	0.4867	0.56553	0.5	Uiso	1
C6	C	0.55636	0.59568	0.5	Uiso	1
C7	C	0.58679	0.55647	0.5	Uiso	1
C8	C	0.5476	0.48684	0.5	Uiso	1
C9	C	0.47797	0.45637	0.5	Uiso	1
C10	C	0.44754	0.49556	0.5	Uiso	1
C11	C	0.57885	0.44663	0.5	Uiso	1
C12	C	0.60508	0.41282	0.5	Uiso	1
C13	C	0.63626	0.37257	0.5	Uiso	1
C14	C	0.70591	0.40299	0.5	Uiso	1
H15	H	0.35695	0.52713	0.5	Uiso	1
H16	H	0.49179	0.66465	0.5	Uiso	1
H17	H	0.58834	0.65248	0.5	Uiso	1
H18	H	0.64359	0.58129	0.5	Uiso	1
H19	H	0.44603	0.39957	0.5	Uiso	1
H20	H	0.39074	0.47073	0.5	Uiso	1
H21	H	0.73792	0.45978	0.5	Uiso	1

Table S4. The photocatalytic performance comparison of EBA-COF and BTEA-COF with other representative materials.

Samples	H_2O_2 Production rate (μmol/h·g)	Irradiation conditions	Solvent	Reference
EBA-COF	1820	λ = 420 nm	H_2O: EtOH (9:1)	This work
	1820		H_2O: Isopropanol (9:1)	
	2550		H_2O: benzyl alcohol (9:1)	
BTEA-COF	780	λ = 420 nm	H_2O: EtOH (9:1)	
TAPD-$(Me)_2$ COF	97.0	λ = 420-700 nm	H_2O: EtOH (9:1)	S6
TAPD-$(OMe)_2$ COF	91.0	λ = 420-700 nm	H_2O: EtOH (9:1)	
CTF-BDDBN	96.7	λ = 420-700 nm	H_2O	S7
CTF-EDDBN	56.7	λ = 420-700 nm	H_2O	
CTF-BPDCN	28.3	λ = 420-700 nm	H_2O	
g-C_3N_4	63.0	λ = 420-500 nm	H_2O: EtOH (1:9)	S8
mesoporous g-C_3N_4	22.5	λ > 420 nm	H_2O: EtOH (1:9)	S9
RF523 resin	51.7	λ > 420 nm	H_2O	S10
TiO_2	7.0	λ > 280 nm	benzyl alcohol and H_2O	S11
PC-HM(g-C_3N_4)	268	λ > 420 nm	benzyl alcohol and H_2O	S12
OCN-500	106	λ > 420 nm	H_2O	S13
g-C_3N_4/PDI51	21	λ > 420 nm	H_2O	S14
g-C_3N_4/PDI/r$GO_{0.05}$	24.2	λ > 420 nm	H_2O	S15
Fe-g-C_3N_4	16	λ > 420 nm	H_2O	S16
g-C_3N_4 aerogels	28.8	λ > 420 nm	H_2O	S17

Section D. References

[S1] T. Weymuth, J. Proppe, M. J. Reiher, Theory Comput., **2018**, *14*, 2480-2494.

[S2] T. Lu, F. Chen, J. Comput. Chem., **2012**, *33*, 580-592.

[S3] S. Wei, F. Zhang, W. Zhang, P. Qiang, K. Yu, X. Fu, D. Wu, S. Bi, F. Zhang, *J. Am. Chem. Soc*. **2019**, *141*, 14272−14279.

[S4] M. Cui, W. Bai, H. H. Y. Sung, I. D. Williams, G. Jia, *J. Am. Chem. Soc*. **2020**, *142*, 13339−13344.

[S5] R. L. Greenaway, V. Santolini, M. J. Bennison, B. M. Alston, C. J. Pugh, M. A. Little, M. Miklitz, E. G. B. Eden-Rump, R. Clowes, A. Shakil, H. J. Cuthbertson, H. Armstrong, M. E. Briggs, K. E. Jelfs, A. I. Cooper, *Nat. Commun*. **2018**, *9*, 2849.

[S6] C. Krishnaraj, H. S. Jena, L. Bourda, A. Laemont, P. Pachfule, J. Roeser, C. V. Chandran, S. Borgmans, S. M. J. Rogge, K. Leus, C. V. Stevens, J. A. Martens, V. V. Speybroeck, E. Breynaert, A. Thomas, P. V. D. Voort, *J. Am. Chem. Soc*. **2020**, *142*, 20107-20116.

[S7] L. Chen, L. Wang, Y. Wan, Y. Zhang, Z. Qi, X. Wu, H. Xu, *Adv. Mater.* **2019**, e1904433.

[S8] Y. Shiraishi, S. Kanazawa, Y. Sugano, D. Tsukamoto, H. Sakamoto, S. Ichikawa, T. Hirai, *ACS Catal.* **2014**, *4*, 774-780.

[S9] Y. Shiraishi, Y. Kofuji, H. Sakamoto, S. Tanaka, S. Ichikawa, T. Hirai, *ACS Catal.* **2015**, *5*, 3058-3066.

[S10] Y. Shiraishi, T. Takii, T. Hagi, S. Mori, Y. Kofuji, Y. Kitagawa, S. Tanaka, S. Ichikawa, T. Hirai, *Nat. Mater*. **2019**, *18*, 985-993.

[S11] Y. Shiraishi, S. Kanazawa, D. Tsukamoto, A. Shiro, Y. Sugano, T. Hirai, *Angew. Chem. Int. Ed*. **2020**, *59*, 17356-17376.

[S12] H. Ou, C. Tang, X. Chen, M. Zhou, X. Wang, *ACS Catal*. **2019**, *9*, 2949-2955.

[S13] Z. Wei, M. Liu, Z. Zhang, W. Yao, H. Tan, Y. Zhu, *Energy Environ. Sci.* **2018**, *11*, 2581-2589.

[S14] Y. Shiraishi, S. Kanazawa, Y. Kofuji, H. Sakamoto, S. Ichikawa, S. Tanaka, T. Hirai, *Angew. Chem. Int. Ed*. **2014**, *53*, 13454-13459.

[S15] Y. Kofuji, Y. Isobe, Y. Shiraishi, H. Sakamoto, S. Tanaka, S. Ichikawa, T. Hirai, *J. Am. Chem. Soc*. **2016**, *138*, 10019-10025.

[S16] X. Chen, J. Zhang, X. Fu, M. Antonietti, X. Wang, *J. Am. Chem. Soc.* **2009**, *131*, 11658-11659.

[S17] H. Ou, P. Yang, L. Lin, M. Anpo, X. Wang, *Angew. Chem. Int. Ed*. **2017**, *56*, 10905-10910.